Assessment of positional reproducibility in the head and neck on a 1.5-T MR simulator for an offline MR-guided radiotherapy solution

Yihang Zhou[1], Jing Yuan[1], Oi Lei Wong[1], Winky Wing Ki Fung[2], Ka Fai Cheng[2], Kin Yin Cheung[1], Siu Ki Yu[1]

[1]Medical Physics and Research Department, [2]Department of Radiotherapy, Hong Kong Sanatorium & Hospital, Hong Kong, China

Correspondence to: Yihang Zhou, PhD. Medical Physics and Research Department, Hong Kong Sanatorium & Hospital, 8/F, Li Shu Fan Block, 2 Village Road, Happy Valley, Hong Kong, China. Email: yihang.zhou@outlook.com.

Background: Recently, a shuttle-based offline magnetic resonance-guided radiotherapy (MRgRT) approach was proposed. This study aims to evaluate the positional reproducibility in the immobilized head and neck using a 1.5-T MR-simulator (MR-sim) on healthy volunteers.

Methods: A total of 159 scans of 14 healthy volunteers were conducted on a 1.5-T MR-sim with thermoplastic mask immobilization. MR images with isotropic 1.05^3 mm^3 voxel size were rigidly registered to the first scan based on fiducial, anatomical and gross positions. Mean and standard deviation of positional displacements in translation and rotation were assessed. Systematic error and random errors of positioning in the head and neck on the MR-sim were determined in the translation of, and in the rotation of roll, pitch and yaw.

Results: The systematic error (Σ) of translation in left-right (LR), anterior-posterior (AP) and superior-inferior (SI) direction was 0.57, 0.22 and 0.26 mm for fiducial displacement, 0.28, 0.10 and 0.52 mm for anatomical displacement, and 0.53, 0.22 and 0.49 mm for gross displacement, respectively. The random error (σ) in corresponding translation direction was 2.07, 0.54 and 1.32 mm for fiducial displacement, 1.34, 0.73 and 2.04 mm for anatomical displacement, and 2.24, 0.86 and 2.61 mm for gross displacement. The systematic error and random error of rotation were generally smaller than 1°.

Conclusions: Our results suggested that high gross positional reproducibility (<1 mm translational and <1° rotational systematic error) could be achieved on an MR-sim for the proposed offline MRgRT.

Keywords: Positional reproducibility; head and neck; magnetic resonance-simulator (MR-sim); immobilization; magnetic resonance-guided radiotherapy (MRgRT)

Introduction

Magnetic resonance imaging (MRI) has attracted greater interest in radiotherapy (RT) applications in recent years (1-8). MRI introduces a number of benefits that may confer an advantage over the conventional use of X-ray based imaging methods in RT, such as non-ionizing radiation, improved soft tissue contrast and multi-planar imaging capability. In recent years, modified clinical wide-bore MRI scanners, named MR-simulator (MR-sim), have been introduced for RT treatment planning purpose. MR-sims enable the use of RT immobilization devices during MR scan to ensure the identical patient positioning of MR scan to that of RT treatment so as to greatly reduce the image registration error to planning CT and thus improve delineation accuracy. In addition, the recent development of the hybrid MR-guided radiotherapy (MRgRT) modalities, such as MR-LINAC (9-11) and MR-Cobalt 60 RT machine (12), further extend the role of MRI in RT from treatment planning to on-board patient positional verification and

real-time treatment delivery guidance and monitoring.

Despite the great technical advantages of hybrid MRgRT modalities capable of online simultaneous MR imaging and radiation delivery, the high cost of machine and siting, the complicated workflow, as well as the unproven clinical value, all hamper the wide use of these MRgRT modalities in normal clinical centers. A complementary approach by using an MR-sim and a patient transfer system has been recently proposed (13,14) as an offline MRgRT solution to greatly reduce the extremely high cost of hybrid MRgRT system while utilizing the superior image quality of MRI for RT guidance. In this approach, a patient receives normal CT and MR simulation scans for treatment planning. During the treatment course, the patient is firstly positioned and receives daily MRI scan on an MR-sim for each treatment fraction. After that, the patient in his/her setup position is transferred to the RT treatment machine via a shuttle-based transfer system. Some commercially available such shuttle systems like the MR-compatible air-bearing Zephyr XL System (Diacor, Salt Lake City, Utah, USA) provide the capability to effortlessly move the patient by a transfer sled from an MR-sim to a treatment machine and minimize the risk of patient positional change during transfer. The patient positioning could be finally verified via laser alignment and/or on-board imaging. Positional correction or re-setup will be triggered on the treatment machine couch if substantial positional difference between daily MRI, on-board imaging and planning CT/MRI is found to exceed the tolerance set for different treatment schemes. Although this offline MRgRT solution is incapable of real-time MR imaging during the radiation delivery, it is postulated that its guidance performance might not be much compromised compared to the hybrid MRgRT system for those relatively stationary tumor sites during treatment such as brain tumor and many head and neck tumors, as long as high patient setup accuracy could be achieved on an MR-sim and the patient positioning could be well maintained during patient transfer.

To validate this offline MRgRT solution and verify its clinical feasibility, investigation of positional repeatability that could be achieved on an MR-sim is essential. Positional repeatability is much dependent on many factors such as the rigidity of patient couch (15), the fixability of immobilization devices (16-18), the accuracy of laser and the set-up skills of radiotherapist, but theoretically independent of imaging technique. However, the different characteristics of MR images from X-ray radiographic images might have potential influence on image co-registration and thus affect the positional repeatability quantification. For example, the positional repeatability derived from X-ray imaging might majorly reflect the alignment of the bony structures since soft tissues are not well visualized (19-21). In contrast, the positional repeatability derived from MRI is postulated to be more affected by various sequence-dependent soft tissue contrasts (22-24). Meanwhile, an MR-sim also has different configurations from the treatment machine. For example, an MR-sim is typically equipped with a patient couch only movable along superior-inferior (SI) direction on a fixed anterior-posterior (AP) height, so has fewer degrees-of-freedom compared to the CT-sim and treatment machines. Therefore, although the positional uncertainty in the head and neck has been extensively investigated using X-ray based imaging (18,19,25-33), these results might not be identical to the MR-derived positional repeatability on an MR-sim.

In this pilot prospective study, we aim to assess the positional reproducibility in the head and neck immobilized with routinely used thermoplastic mask in RT in a group of healthy volunteers on an RT-dedicated 1.5T MR-simulator.

Methods

This study was approved by the institutional research ethics committee. A total of 14 healthy volunteers, aged between 24 and 40 years, were recruited for this study. Informed consent was obtained from each subject.

Scan setup and data acquisition

MR images were acquired on a 1.5-Tesla MR-sim (Aera, Siemens Healthineers, Erlangen, Germany) dedicated for RT applications. All volunteers were lied on a MR-compatible RT flat coach top (Diacor, Salt Lake City, Utah, USA) overlaid on the MR-sim patient table, and then immobilized using a customized head-and-neck and shoulder thermoplastic mask (Orfit Industries, Belgium) and a standard neck rest. Permanent lines were drawn on the thermoplastic mask before the first scan session for future positioning reference with the aid of a well-calibrated 3-dimensional external laser system (DORADOnova MR3T, LAP GmbH Laser Applikationen, Luneburg, Germany). MR-CT visible fiducial markers (PinPoint, Beekley Medical, USA) were attached on the drawn lines on the thermoplastic mask. After the alignment to the drawn lines on the mask using the external laser, two flexible 4-channel surface coils were wrapped around the
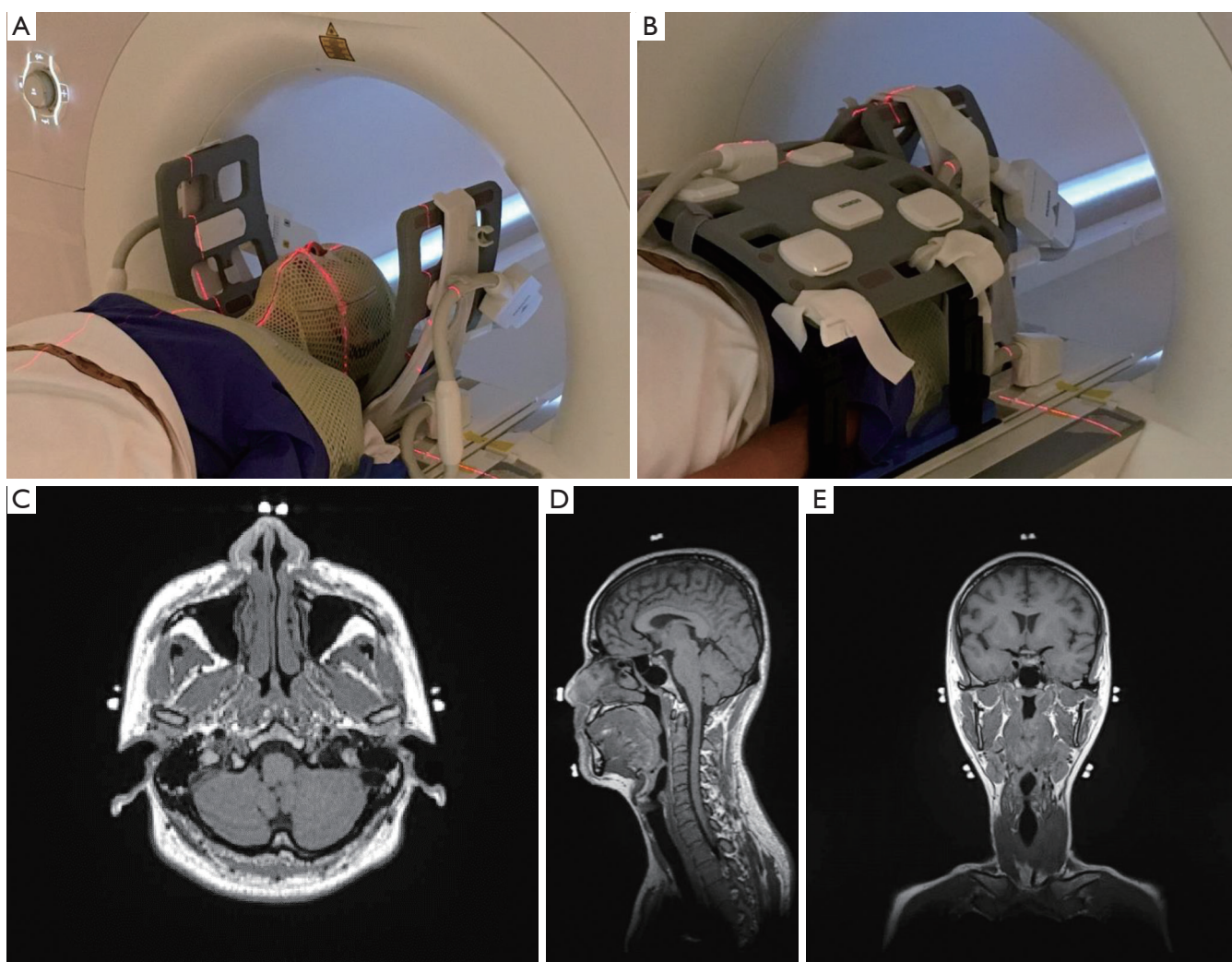
Figure 1 Illustration of a subject positional verification setup and the acquired 3D high resolution MR images. (A) Demonstration of a subject immobilized using thermoplastic mask aligned with the external laser system; (B) demonstration of a subject setup and the coil setting on the MR-sim; (C-E) one representative slice of axial, sagittal and coronal view of the acquired 3D MR image from one of the subjects.

head without touching using two customized bi-lateral coil holders (Orfit Industries, Belgium). An 18-channel flexible body coil was positioned as close as possible to the subject but without touching the subject by using two coil bridges (Orfit Industries, Belgium) to cover the anterior neck and chest for acquisition. Embedded spine coil array of the MR-sim underneath the flat couch-top were used to cover the posterior neck and chest for acquisition. A typical volunteer setup that was immobilized and aligned with external laser system is illustrated in *Figure 1*.

Each volunteer received a series of scans on the MR-sim in an RT treatment position to simulate the HNC RT treatment fractions. Among them, three volunteers received

40, 38 and 32 fractions, respectively, within one month; two volunteers received 6 and 7 fractions, respectively, within 1 week, and the rest nine volunteers received 4 fractions within 1 day. In total, 159 imaging fractions were conducted. Each volunteer was carefully positioned and aligned for each scan session. The imaging protocol consisted of a T1-weighted Sampling Perfection with Application optimized Contrasts using different flip angle Evolution (SPACE) sequence [FOV =470 mm (LR, phase-encoding direction) ×470 mm (SI, frequency-encoding direction) ×269 mm (AP, slice-encoding direction), matrix size =448 (LR)×448 (SI)×256 (AP), that yielded an isotropic voxel size of 1.05×1.05×1.05 mm³; TR/TE =420/7.2 ms,

928

Zhou et al. Head-and-neck positional reproducibility on a 1.5-T MR simulator

echo train length (ETL) =40, iPAT factor (GRAPPA) =3, slice-encoding partial Fourier factor =6/8, Bandwidth =657 Hz/pixel, acquisition time =5 min 1 sec]. Receive B1 field inhomogeneity correction technique, i.e., pre-scan normalization, was applied to minimize the MR image intensity non-uniformity. Console-integrated 3D geometric distortion correction was also enabled to minimize MR image distortion.

Data analysis

All acquired MR data were exported as DICOM images and processed offline using 3D Slicer version 4.5.0 (http://www.slicer.org). Three sets of image registration were conducted using 6 degree-of-freedom (DOF) rigid body registration based on normalized mutual information. The first set of registration was named fiducial registration to assess the alignment accuracy during subject setup. In this procedure, the fiducial markers on the thermoplastic mask were manually segmented on MR images, and pair-wisely registered with respect to the first session for each subject. The second registration set was named anatomical registration to assess the anatomical motion induced positional variation under the thermoplastic mask excluding the effect of fiducial alignment uncertainty. In this registration, the fiducial-registered MR images were further rigidly registered with respect to the first session based purely on anatomical information. Five percent of anatomical image voxels were randomly sampled for this registration. The third registration was named gross registration to assess the gross subject positional repeatability. In this registration, the fiducial markers were manually removed from all original MR images to completely avoid the chance of selecting fiducial marker voxels in image registration. Then, head and neck anatomies (5% voxels sampling) were pair-wisely registered with respect to the first session for each subject. For all three registrations, the output transformation matrices were recorded to calculate the translation in left-right (LR), AP and SI directions and the rotation in roll, pitch and yaw directions. Translation to right, anterior and superior direction and rotation to the clock-wise direction were defined as positive.

Statistical method

Shapiro-Wilk test was used to test the normality of the displacement distribution in the translation and rotation directions.

Systematic and random errors in translation and rotation were calculated. In this study, the group mean error (M) was defined as the mean of all mean displacements for all subjects. The systematic error (Σ) was defined as the standard deviation (SD) of the mean displacement in the subject group. The random error (σ) was defined by the root mean square of the standard deviation of the position displacement in all subjects.

Student t-test and analysis of variance (ANOVA) were used to assess the inter-subject positional variation in the translation and rotation directions from the abovementioned three different registration strategies. A P value of 0.05 or smaller was considered statistically significant.

Results

Translational and rotational displacement

Figure 2 shows the average translation in LR, AP and SI and rotation in roll, pitch and yaw of all subjects derived from the three registrations. Shapiro-Wilk test showed that all displacements in translations and rotations followed the normal distribution (P>0.05). Table 1 presented the average displacements and standard deviation of translation in LR, SI and AP and rotation in roll, pitch and yaw using three registration methods. Averaged across the total 159 imaging sessions, 18/159 (11.3%), 1/159 (0.6%), and 10/159 (6.3%) in LR, and 4/159 (2.5%), 6/159 (3.8%) and 10/159 (6.3%) in SI of all sessions had the displacement >1 mm from fiducial, anatomical and gross registration, respectively. No sessions had the displacement >1 mm in AP. The displacement over 2 mm was only observed in SI once (1/159, 0.6%) from gross registration. Figure 3 shows the box-plot of group's inter-sessional translation and rotation. Student t-test showed significant differences between LR and AP (P=0.01), AP and SI (P<0.001), as well as LR and SI (P=0.021) from anatomical registration; LR and AP (P=0.014), and AP and SI (P<0.001) from gross registration; and in all rotations (P<0.001) from three registration methods except for roll and pitch from gross registration. The group's inter-methodological translation and rotation box-plot are presented in Figure 4. Significant differences were observed in translation (P<0.02) and rotation (P<0.004) in all directions from three registration methods except for the translation in LR between fiducial and anatomical/gross registrations, rotation in pitch between gross and fiducial/anatomical registrations, and rotation in yaw between gross
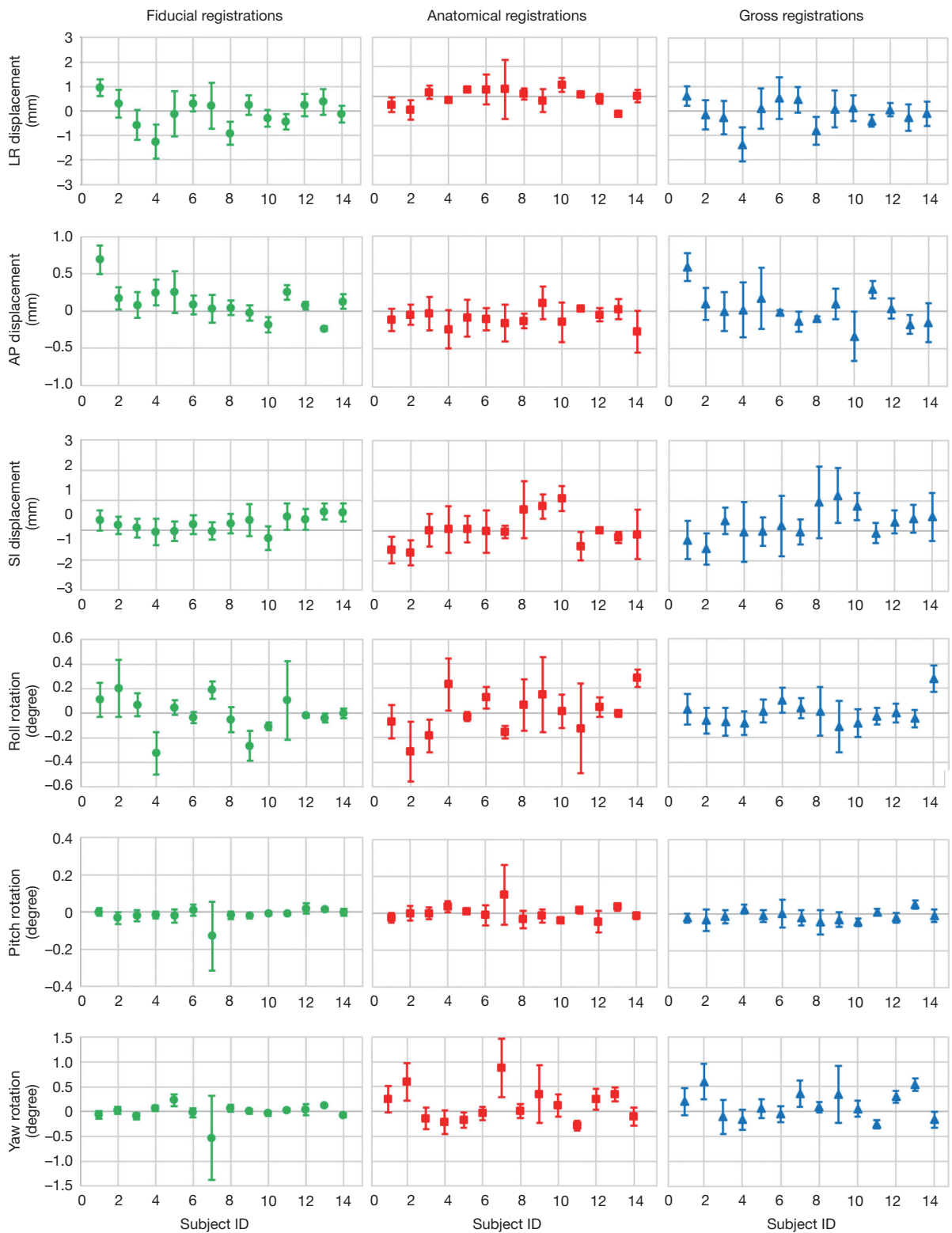
Figure 2 Average translations in LR, AP and SI and rotations in roll, pitch and yaw of all subjects based on fiducial, anatomical and gross registrations. Error bar represents the standard deviation.

Table 1 Average displacements and standard deviation of translation in LR, SI and AP directions and rotation in roll, pitch and yaw directions using three registration methods

Registration methods	3D translation			3D rotation		
	LR	AP	SI	Roll	Pitch	Yaw
Fiducial registration (mm)						
Mean	0.14	0.27	0.21	0.08	0.00	−0.03
SD	0.81	0.32	0.34	0.20	0.00	0.16
Anatomical registration (mm)						
Mean	−0.17	−0.08	−0.31	−0.12	0.00	0.21
SD	0.38	0.19	0.65	0.24	0.00	0.42
Gross registration (mm)						
Mean	0.01	0.17	−0.07	−0.02	0.00	0.21
SD	0.73	0.34	0.73	0.13	0.00	0.41
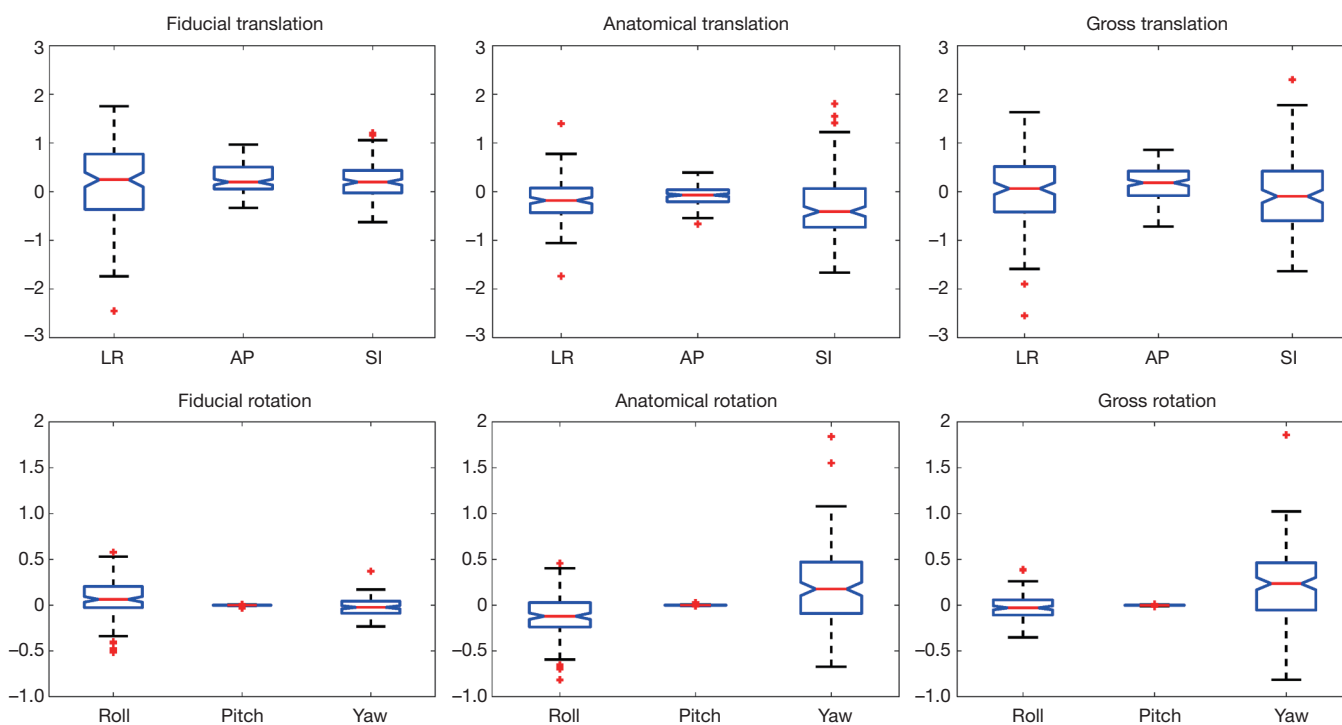
Figure 3 Box-plot of group's inter-sessional translations and rotations based on fiducial (left), anatomical (middle) and gross (right) registrations.

and anatomical registrations.

Systematic and random error

The calculated systematic and random errors are summarized in *Table 2*. The systematic error (Σ) of translation in LR, AP and SI was 0.57, 0.22 and 0.26 mm for fiducial displacement, 0.28, 0.10 and 0.52 mm for anatomical displacement, and 0.53, 0.22 and 0.49 mm for gross displacement, respectively. The systematic error
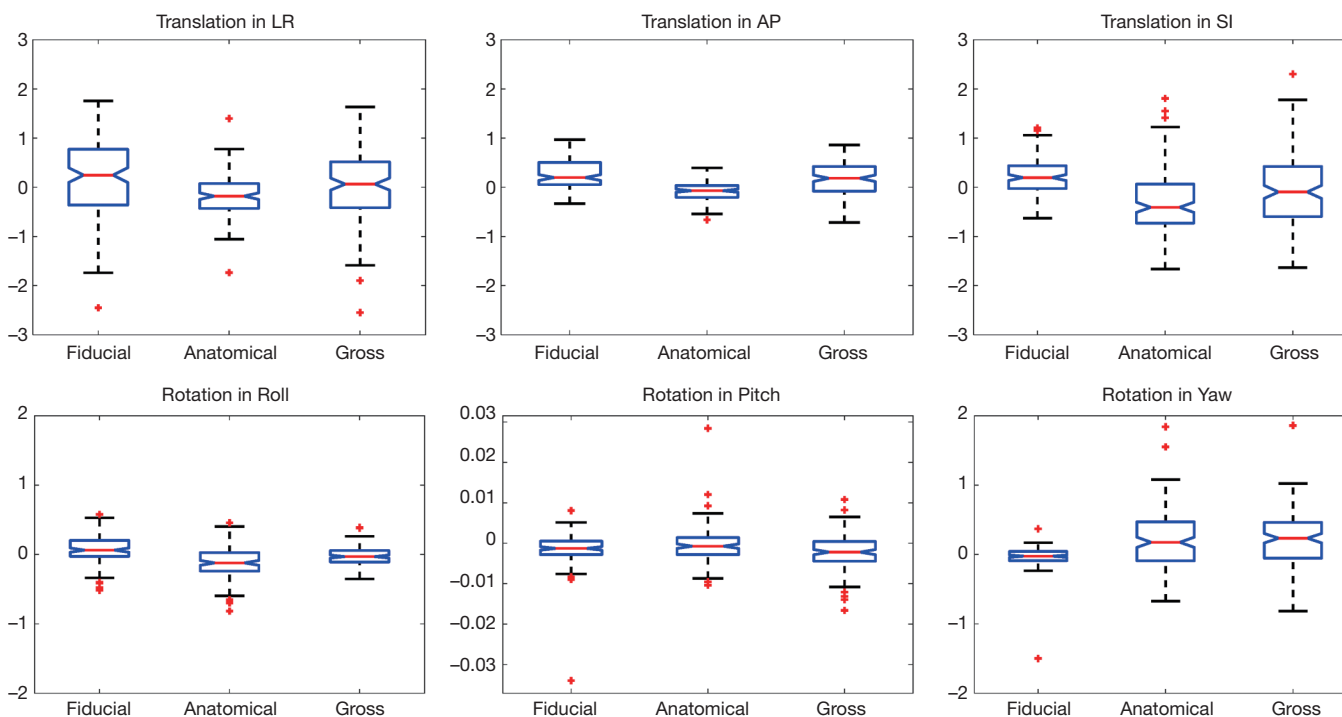
Figure 4 Box-plot of group's inter-methodological translation and rotation displacements.

Table 2 Calculated systematic and random errors in 3D translation and rotation using three registration methods

Registration methods	3D translation			3D rotation		
	LR (mm)	AP (mm)	SI (mm)	Roll (°)	Pitch (°)	Yaw (°)
Fiducial registration						
Group mean error M	−0.08	0.11	0.21	−0.01	0.00	−0.01
Systematic error Σ	0.57	0.22	0.26	0.15	0.00	0.17
Random error σ	2.07	0.54	1.32	0.50	0.02	0.88
Anatomical registration						
Group mean error M	−0.03	−0.08	0.03	0.00	0.00	0.13
Systematic error Σ	0.28	0.10	0.52	0.17	0.00	0.33
Random error σ	1.34	0.73	2.04	0.67	0.02	1.10
Gross registration						
Group mean error M	−0.10	0.03	0.25	0.00	0.00	0.13
Systematic error Σ	0.53	0.22	0.49	0.10	0.00	0.27
Random error σ	2.24	0.86	2.61	0.44	0.02	0.95

(Σ) of rotation in roll, pitch and yaw was 0.15°, 0.00° and 0.17° for fiducial displacement, 0.17°, 0.00° and 0.33° for anatomical displacement, and 0.10°, 0.00° and 0.27° for gross displacement, respectively. The group random error (σ) in corresponding translation direction was 2.07, 0.54 and 1.32 mm for fiducial displacement, 1.34, 0.73

and 2.04 mm for anatomical displacement, and 2.24, 0.86 and 2.61 mm for gross displacement. The group random error (σ) in corresponding rotation was 0.50°, 0.02° and 0.88° for fiducial displacement, 0.67°, 0.02° and 1.10° for anatomical displacement, and 0.44°, 0.02° and 0.95° for gross displacement, respectively.

Discussion

In this prospective study, we quantitatively assessed the positional repeatability in the head and neck on a group of healthy volunteers using a 1.5-T MR-sim with RT routinely used thermoplastic mask immobilization for a recently proposed offline MTgRT solution. In particular, we comprehensively evaluated the positioning error introduced by thermoplastic mask immobilization, anatomical motion and the resultant gross subject positional repeatability.

In general, high accuracy of setup alignment was achieved on the MR-sim as revealed by the sub-millimeter translational systematic error of fiducial registration. The random error σ of translational fiducial registration was largest in LR and smallest in AP. Since the scan on the MR-sim could only be conducted on a fixed height in AP, the AP alignment during setup on the MR-sim was no longer needed. Considering the thickness (~1 mm) of the drawn line for alignment on the mask and the smallest moving increment of 1 mm of the MRI couch, the random error of fiducial registration in SI (1.32 mm) was reasonable. The relatively large random error of fiducial registration in LR (2.07 mm) might attribute to the thermoplastic mask deformability as well as the slightly loose LR fixation of the MRI couch on its sliding track. In this aspect, the mechanical fixation in LR of the MR-sim should be further improved. The anatomical registration mainly revealed the anatomy motion under the thermoplastic mask immobilization independent of fiducial alignment during setup. In general, the translational systematic error of anatomical registration was smaller than 1 mm as well. Compared with fiducial registration, the random error in LR (1.34 mm) of anatomical registration was smaller, while in SI (2.04 mm) was larger, indicating the relatively large anatomical mobility in this direction. By taking into account of both effects of fiducial alignment accuracy and anatomy mobility under the thermoplastic mask immobilization, the gross registration revealed the overall positional repeatability that could be achieved on the MR-sim. The random error was worst in SI (2.61 mm), best in AP (0.86 mm) and in-between in LR (2.24 mm). The systematic

error of gross registration still well remained within 1 mm, indicating the high overall positional accuracy achieved on the MR-sim.

Setup uncertainties in head and neck have been assessed in many studies using X-ray based radiographic image guided radiation therapy (IGRT). Gupta et al. (31) reported the 3-dimensional systematic and random errors in conventional head and neck RT using electronic portal imaging were 0.96, 0.98 and 1.20 mm and 1.97, 1.94 and 2.48 mm in LR, AP and SI direction respectively. Xu et al. (25) reported for head and neck tumors, the inter-fractional setup errors on LR, AP and SI using CBCT were 1.2±0.9, 1.2±1.1 and 1.0±0.8 mm, respectively; Qi et al. (29) reported that the inter-session displacements of setup error in LR, AP, and SI for three CT-based IGRT systems were 0.5±1.5, 0.3±1.7 and –0.3±2.0 mm (KV cone beam CT, KVCBCT); 0.2±1.9, 0.0±1.7, and –0.2±2.4 mm (MV fan beam CT, MVFBCT); and 0.0±1.8, 0.8±3.0, and 0.5±1.7 mm (MV cone beam CT, MVCBCT). The random errors for KVCBCT, MVFBCT, and MVCBCT were 1.4–1.6, 1.7, and 2.0–2.1 mm.

It is of value to illustrate the characteristics of MR-derived gross positional repeatability in this study by comparing to those derived from CT-based studies. In our study, the systematic errors of gross positional repeatability were well below 1 mm in translation and 0.1 degree in rotation, indicating the high accuracy of head and neck positioning with thermoplastic mask immobilization on the MR-sim. Meanwhile, there was no trend of translational and rotational drift between multiple scan sessions to introduce increase in systematic errors. In addition, systematic errors were generally smaller than the random errors, which was also consistent with those CT studies. However, our result showed a similar setup error in LR and SI, but a smaller setup error in AP compared to those CT-based studies.

A number of factors may attribute to these differences. Firstly, our study was based on a group of healthy volunteers rather than real HNC patients. For healthy volunteers, much smaller inter-sessional anatomic change, such as weight loss, can be presumed. Meanwhile, healthy volunteers should have better keeping-still and motion control capability compared to real patients. These both account for the smaller setup error revealed in our study.

Secondly, the MR-sim couch is only movable in SI at a fixed AP height while modern RT machines are usually equipped with a 6-degree-of-freedom patient couch. This might partially explain the smaller AP displacement in our study. It is observed that the gross translational random

error of LR translation (2.61 mm) in our study was slightly larger than the reported values by using radiographic images, partially attributed to the slightly loose LR fixation of the MRI couch.

Thirdly, different image characteristics between X-ray based imaging and MRI and their influences on image registration should be considered. Positional verification in the current RT practice relies heavily on bony structure registration using the X-ray based images. The influence of soft tissue anatomies on image registration for positional verification is very small as they are usually poorly visualized on X-ray based images. In contrast, MRI provides much better soft-tissue contrast, in particular for target tumors and adjacent critical tissues. MR image registration procedure utilized both soft tissue and hard tissue anatomies. As such, smaller registration errors and uncertainties could be postulated (21), and the results might more accurately reveal the true inter-sessional positioning repeatability. It is also worth noting that high-resolution isotropic voxel-size MR images were acquired in this study to minimize registration bias, uncertainty and error.

This study has limitations. First, this study only included a small number of healthy volunteers. Positional variability might be underestimated in healthy volunteer data in the absence of inter-fractional anatomical variation due to patient weight loss, tumor shrink, and other tissue deformations during treatment. The small number of subjects limited the statistical power of the analysis. Meanwhile, three subjects accounted for 69.1% (110/159) of all scan sessions. These highly skewed data, although helpful to more accurately assess the inter-sessional variability, might adversely introduce the bias in the result of inter-subject variability. Second, to acquire isotropic high-resolution 3D images, the MR scan time (~5 min) was much longer than the positional verification imaging protocol in the common RT practice. To translate it into positional verification practice of the proposed offline MRgRT approach, smaller image volume and/or larger voxel size should be adopted to greatly reduce the scan time. Last but not least, the residual MR image geometric distortion after applying geometric distortion was not accounted for and its potential influence on positional repeatability was not investigated.

Future research work is warranted for applying offline MRgRT in practice. First, in addition to the gross positional repeatability assessed on the MR-sim, the positional variation due to the patient transfer procedure should be rigorously investigated as well. Otherwise, the high positional repeatability achieved on the MR-sim could not be guaranteed on the treatment machine couch. Secondly, the gross positional repeatability did not sufficiently and faithfully reveal the regional and localized positional repeatability of different soft tissues due to their variability in mobility and deformability. MRI provides the possibility for MRgRT to build positional verification protocol based directly on target tumor and/or soft tissues instead of bony structure surrogates. Therefore, optimized patient setup, positional verification and correction strategies need to be further explored for this purpose. Thirdly, the influences of different MRI pulse sequences and different imaging parameters are to be evaluated for positional verification. Furthermore, multi-modality imaging registration uncertainty should also be rigorously determined particularly for MR guided radiosurgery applications in which high precision is critically required. Last but not least, regular quality assurance of MR imaging (34) on an MR-sim is yet to be developed and established.

Conclusions

In this pilot study, we measured the systematic and random errors of positional reproducibility in the head and neck with immobilization using a 1.5-T MR-sim. Our results suggested that high gross positional reproducibility (<1 mm translational and <1° rotational systematic error) could be achieved on an MR-sim for the newly proposed offline MRgRT solution.

Acknowledgements

Footnote

Conflicts of Interest: The authors have no conflicts of interest to declare.

Ethical Statement: This study was approved by the Institutional Research Ethics Committee (RC-2015-08) and written informed consent was obtained from all subjects.

References

1. Buhl SK, Duun-Christensen AK, Kristensen BH, Behrens CF. Clinical evaluation of 3D/3D MRI-CBCT automatching on brain tumors for online patient setup

verification–A step towards MRI-based treatment planning. Acta Oncologica 2010;49:1085-91.

2. Karlsson M, Karlsson MG, Nyholm T, Amies C, Zackrisson B. Dedicated magnetic resonance imaging in the radiotherapy clinic. Int J Radiat Oncol Biol Phys 2009;74:644-51.

3. Nyholm T, Jonsson J. Counterpoint: opportunities and challenges of a magnetic resonance imaging–only radiotherapy work flow. Semin Radiat Oncol 2014;24:175-80.

4. Lee YK, Bollet M, Charles-Edwards G, Flower MA, Leach MO, McNair H, Moore E, Rowbottom C, Webb S. Radiotherapy treatment planning of prostate cancer using magnetic resonance imaging alone. Radiother Oncol 2003;66:203-16.

5. Prabhakar R, Julka PK, Ganesh T, Munshi A, Joshi RC, Rath GK. Feasibility of using MRI alone for 3D radiation treatment planning in brain tumors. Jpn J Clin Oncol 2007;37:405-11.

6. Jonsson JH, Karlsson MG, Karlsson M, Nyholm T. Treatment planning using MRI data: an analysis of the dose calculation accuracy for different treatment regions. Radiat Oncol 2010;5:62.

7. Sykes JR, Brettle DS, Magee DR, Thwaites DI. Investigation of uncertainties in image registration of cone beam CT to CT on an image-guided radiotherapy system. Phys Med Biol 2009;54:7263-83.

8. Gurney-Champion OJ, McQuaid D, Dunlop A, Wong KH, Welsh LC, Riddell AM, Koh DM, Oelfke U, Leach MO, Nutting CM, Bhide SA, Harrington KJ, Panek R, Newbold KL. MRI-based Assessment of 3D Intrafractional Motion of Head and Neck Cancer for Radiation Therapy. Int J Radiat Oncol Biol Phys 2018;100:306-16.

9. Lagendijk JJ, Raaymakers BW, Raaijmakers AJ, Overweg J, Brown KJ, Kerkhof EM, van der Put RW, Hårdemark B, van Vulpen M, van der Heide UA. MRI/linac integration Radiother Oncol 2008;86:25-9.

10. Lagendijk JJ, Raaymakers BW, Van Vulpen M. The magnetic resonance imaging–linac system. Semin Radiat Oncol 2014;24:207-9.

11. Metcalfe P, Liney GP, Holloway L, Walker A, Barton M, Delaney GP, Vinod S, Tome W. The potential for an enhanced role for MRI in radiation-therapy treatment planning. Technol Cancer Res Treat 2013;12:429-46.

12. Mutic S, Dempsey JF. The ViewRay system: magnetic resonance-guided and controlled radiotherapy. Semin Radiat Oncol 2014;24:196-9.

13. Bostel T, Pfaffenberger A, Delorme S, Dreher C, Echner G, Haering P, Lang C, Splinter M, Laun F, Müller M, Jäkel O, Debus J, Huber P, Sterzing F, Nicolay N. Prospective feasibility analysis of a novel off-line approach for MR-guided radiotherapy. Strahlenther Onkol 2018;194:425-434.

14. Bostel T, Nicolay NH, Grossmann JG, Mohr A, Delorme S, Echner G, Häring P, Debus J, Sterzing F. MR-guidance-a clinical study to evaluate a shuttle- based MR-linac connection to provide MR-guided radiotherapy. Radiat Oncol 2014;9:12.

15. Schmidhalter D, Malthaner M, Born EJ, Pica A, Schmuecking M, Aebersold DM, Fix MK, Manser P. Assessment of patient setup errors in IGRT in combination with a six degrees of freedom couch. Z Med Phys 2014;24:112-22.

16. Gilbeau L, Octave-Prignot M, Loncol T, Renard L, Scalliet P, Grégoire V. Comparison of setup accuracy of three different thermoplastic masks for the treatment of brain and head and neck tumors. Radiother Oncol 2001;58:155-62.

17. Halperin R, Roa W, Field M, Hanson J, Murray B. Setup reproducibility in radiation therapy for lung cancer: a comparison between T-bar and expanded foam immobilization devices. Int J Radiat Oncol Biol Phys 1999;43:211-6.

18. Nakata A, Tateoka K, Fujimoto K, Saito Y, Nakazawa T, Abe T, Yano M, Sakata K. The reproducibility of patient setup for head and neck cancers treated with image-guided and intensity-modulated radiation therapies using thermoplastic immobilization device. Int J Med Phys Clin Eng Radiat Oncol 2013;2:117-124.

19. Li XA, Qi XS, Pitterle M, Kalakota K, Mueller K, Erickson BA, Wang D, Schultz CJ, Firat SY, Wilson JF. Interfractional variations in patient setup and anatomic change assessed by daily computed tomography. Int J Radiat Oncol Biol Phys 2007;68:581-91.

20. van Kranen S, van Beek S, Rasch C, van Herk M, Sonke JJ. Setup uncertainties of anatomical sub-regions in head-and-neck cancer patients after offline CBCT guidance. Int J Radiat Oncol Biol Phys 2009;73:1566-73.

21. Morrow NV, Lawton CA, Qi XS, Li XA. Impact of computed tomography image quality on image-guided radiation therapy based on soft tissue registration. Int J Radiat Oncol Biol Phys 2012;82:e733-8.

22. Gurney-Champion OJ, Versteijne E, van der Horst A, Lens E, Rütten H, Heerkens HD, Paardekooper GMRM, Berbee M, Rasch CRN, Stoker J, Engelbrecht MRW, van Herk M, Nederveen AJ, Klaassen R, van Laarhoven

HWM, van Tienhoven G, Bel A. Addition of MRI for CT-based pancreatic tumor delineation: A feasibility study. Acta Oncol 2017;56:923-30.

23. Rasch CR, Steenbakkers RJ, Fitton I, Duppen JC, Nowak PJ, Pameijer FA, Eisbruch A, Kaanders JH, Paulsen F, van Herk M. Decreased 3D observer variation with matched CT-MRI, for target delineation in nasopharynx cancer. Radiat Oncol 2010;5:21.

24. Rasch C, Keus R, Pameijer FA, Koops W, de Ru V, Muller S, Touw A, Bartelink H, van Herk M, Lebesque JV. The potential impact of CT-MRI matching on tumor volume delineation in advanced head and neck cancer. Int J Radiat Oncol Biol Phys 1997;39:841-8.

25. Xu F, Wang J, Bai S, Xu QF, Shen YL, Zhong RM. Interfractional and intrafractional setup errors in radiotherapy for tumors analyzed by cone-beam computed tomography. Ai Zheng 2008;27:1111-6.

26. Kang H, Lovelock DM, Yorke ED, Kriminiski S, Lee N, Amols HI. Accurate positioning for head and neck cancer patients using 2D and 3D image guidance. J Appl Clin Med Phys 2010;12:3270.

27. Bylund KC, Bayouth JE, Smith MC, Hass AC, Bhatia SK, Buatti JM. Analysis of interfraction prostate motion using megavoltage cone beam computed tomography. Int J Radiat Oncol Biol Phys 2008;72:949-56.

28. Nyarambi I, Chamunyonga C, Pearce A. CBCT image guidance in head and neck irradiation: the impact of daily and weekly imaging protocols. J Radiother Pract 2015;14:362-9.

29. Qi XS, Hu AY, Lee SP, Lee P, DeMarco J, Li XA, Steinberg ML, Kupelian P, Low D. Assessment of interfraction patient setup for head-and-neck cancer

intensity modulated radiation therapy using multiple computed tomography-based image guidance. Int J Radiat Oncol Biol Phys 2013;86:432-9.

30. Kapanen M, Laaksomaa M, Tulijoki T, Peltola S, Wigren T, Hyödynmaa S, Kellokumpu-Lehtinen PL. Estimation of adequate setup margins and threshold for position errors requiring immediate attention in head and neck cancer radiotherapy based on 2D image guidance. Radiat Oncol 2013;8:212.

31. Gupta T, Chopra S, Kadam A, Agarwal JP, Devi PR, Ghosh-Laskar S, Dinshaw KA. Assessment of three-dimensional set-up errors in conventional head and neck radiotherapy using electronic portal imaging device. Radiat Oncol 2007;2:44.

32. Li H, Zhu XR, Zhang L, Dong L, Tung S, Ahamad A, Chao KC, Morrison WH, Rosenthal DI, Schwartz DL, Mohan R. Comparison of 2D radiographic images and 3D cone beam computed tomography for positioning head-and-neck radiotherapy patients. Int J Radiat Oncol Biol Phys 2008;71:916-25.

33. Den RB, Doemer A, Kubicek G, Bednarz G, Galvin JM, Keane WM, Xiao Y, Machtay M. Daily image guidance with cone-beam computed tomography for head-and-neck cancer intensity-modulated radiotherapy: a prospective study. Int J Radiat Oncol Biol Phys 2010;76:1353-9.

34. Wong OL, Yuan J, Yu SK, Cheung KY. Image quality assessment of a 1.5T dedicated magnetic resonance-simulator for radiotherapy with a flexible radio frequency coil setting using the standard American College of Radiology magnetic resonance imaging phantom test. Quant Imaging Med Surg 2017;7:205-14.